# Active Site Pressurization: A New Tool for Structure-Guided Drug Design and Other Studies of Protein Flexibility

Ian M. Withers, Michael P. Mazanetz, Hao Wang, Peter M. Fischer, and Charles A. Laughton*

School of Pharmacy and Centre for Biomolecular Sciences, University of Nottingham, Nottingham NG7 2RD, U.K.

Received December 21, 2007

We present a new molecular dynamics methodology to assist in structure-based drug design and other studies that seek to predict protein deformability. Termed Active Site Pressurization (ASP), the new methodology simply injects a resin into the ligand binding-site of a protein during the course of a molecular dynamics simulation such that novel, energetically reasonable protein conformations are generated in an unbiased way that may be better representations of the ligand binding conformation than are currently available. Here we apply two different versions of the ASP methodology to three proteins, cytochrome P450cam, PcrA helicase, and glycogen synthase kinase 3$\beta$ (GSK3$\beta$), and show that the method is capable of inducing significant conformational changes when compared to the X-ray crystal structures. Application of the ASP methodology therefore provides a view of binding site flexibility that is a rich source of data for inclusion in a variety of further investigations, including high-throughput virtual screening, lead hopping, revealing alternative modes of deformation, and revealing hidden exit and entrance tunnels.

## 1. INTRODUCTION

It is widely accepted that one of the principal limitations of current approaches to structure-based drug design is our inability to deal with the phenomenon of induced fit, in particular the fact that the target (protein) site may be able to distort in as yet unobserved ways to accommodate a novel ligand. Over recent years, a variety of different methods have emerged that attempt to deal with this problem; however, most suffer from some shortcomings (for a recent review of current docking methods see ref 1). Some methods rely on some separate process, for example a molecular dynamics (MD) simulation on the apo-form of the protein,[2] to generate an ensemble of conformations that may be docked against. These approaches suffer from the fact that they are a) computationally intensive and b) there is no particular driving force for the protein to deform in the way that an arbitrary ligand might require. Other methods attempt to include protein reorganization on the fly during the docking of each ligand.[3] The problem here is that the computational load is again very high, so short cuts such as only allowing for side chain flexibility may be required for satisfactory performance.

Here we describe the development, and application, of an alternative approach, which we call Active Site Pressurization (ASP). ASP predicts energetically reasonable pathways through which binding sites in proteins may distort and distend to accommodate ligands. The method has the advantage that it does not require any a priori assumptions about the chemical structures of any ligands and results in a view of binding site flexibility that is a rich source of data for inclusion in a variety of further investigations, not just limited to high-throughput virtual screening. The idea behind ASP is that we simulate the process of injecting a resin into the ligand binding site producing a cast, a negative impression of the shape of the site. The novel aspect of ASP is that, as the name suggests, we can force the resin in under a controllable pressure, determined by the force acting upon the resin, so that the binding site is encouraged to distend, in whatever manner is most energetically favorable. We can choose to terminate the process once a target pressure is reached or once the cast has reached a target volume. We can then employ the distended protein structure in conventional screening procedures, and the cast too may be used in alternative ligand design and discovery methods. The ASP approach has been inspired in part by the work of Goodfellow et al.,[4] who developed a modeling method to promote the unfolding of proteins by pumping water molecules into interfaces.

## 2. METHODS

**2.1. Active Site Pressurization Methodology.** We have implemented two prototype versions of ASP within the framework of the AMBER7 molecular simulation package.[5] The first is illustrated diagrammatically in Figure 1. Here the resin takes the form of a rectangular block of noncharged Lennard-Jones (LJ) particles arranged on a regular 3-dimensional grid. The block is overlaid onto the ligand binding site and made big enough to extend beyond the region of interest of the target protein. Initially there are no clashes between the block and the protein because all interactions between the LJ particles in the block and the protein are switched off, i.e. they do not interact with any other atoms in the system. LJ particles located within the active site region are then turned on, i.e. they now interact with the other atoms in the system. When filling the active site, particles are only turned on if the addition of the particle does not result in a steric clash (Figure 1(a)). After filling

* Corresponding author e-mail: charles.laughton@nottingham.ac.uk.

10.1021/ci7004725 CCC: $40.75 
Published on Web 06/14/2008

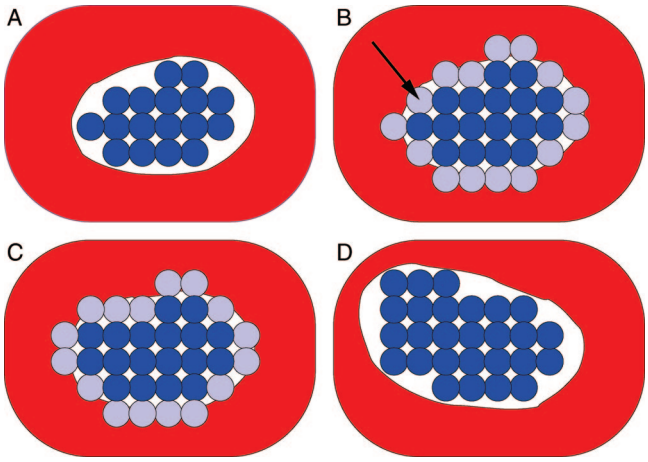


**Figure 1.** Principle of the grid-based version of ASP. A: The active site cavity in the relaxed structure of the protein is filled with LJ particles arrayed on a grid. B: Neighboring particles (light blue) are invisible to the protein but monitor the forces they would experience due to interactions with protein atoms. C: The receptive LJ particle exhibiting the lowest average repulsive force (arrowed in panel B) is switched on and new receptive neighbors identified. D: The process continues, distending the protein active site, until a threshold based on size or repulsive force is reached.

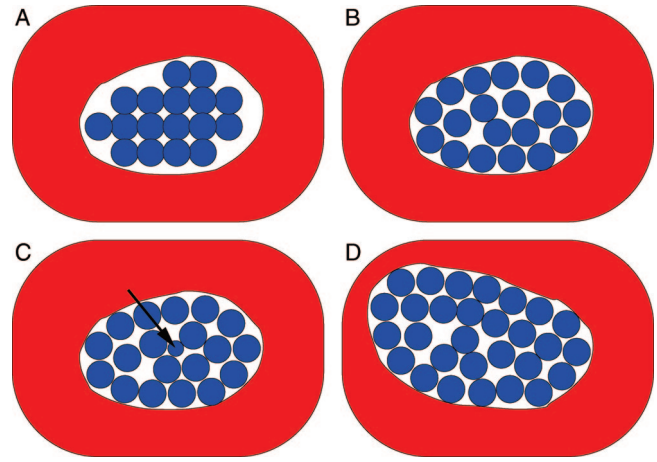


**Figure 2.** The fluid implementation of the ASP procedure. A: The active site cavity in the relaxed structure of the protein is filled with LJ particles arrayed on a grid but not restrained to it. B: Over a short MD trajectory the LJ fluid adapts to the shape of the cavity. C: A new LJ particle is inserted near the center of the fluid mass. Its van der Waals parameters are grown over the course of a short MD trajectory according to eqs 1 and 2. D: The process continues, distending the protein active site, until a threshold based on size is reached.

the active site with particles, all the particles located on grid points neighboring an on particle are flagged as receptive (Figure 1(b)). MD simulations are now performed with the protein responding to any forces it experiences due to the on particles, and the receptive sites monitoring the force they would experience due to the protein, had they been on. After integrating over a suitable time frame, the receptive particle that has experienced the lowest average repulsive force from the protein is switched on. The list of receptive particles is then updated to add the neighbors of this new point (Figure 1(c)), and the MD continues. In this manner the addition of particles will begin to distend the cavity. As new particles are switched on at the sites experiencing the lowest force due to the protein, the protein naturally distorts in the most energetically reasonable manner (Figure 1(d)).

The choice of nonbonded parameters for the LJ particles and grid spacing are important as there are a number of factors that will affect the stability and usefulness of the method. The attractive well-depth does not want to be too strong, otherwise the protein of interest may be deformed in an undesirable manner due to strong interactions between the protein and the LJ particles. In this work the well depth of interactions between LJ particles was set to 0.1 kcal/mol. The equilibrium distance between LJ particles was set to 1.4 Å. The interaction parameters between the LJ particles and other atoms were determined using standard mixing rules.[6] The spacing of the LJ particles on the grid is also important as the use of too small a grid spacing could result in small cavities being explored that realistic ligands would not be able to enter. Too large a grid spacing could result in interesting features in the active site not being explored and also increase the risk of steric overlaps when turning on receptive particles. Following a number of preliminary simulations a grid spacing of 1.1 Å was chosen. These preliminary simulations also showed that stable behavior is observed when a particle is turned on every 2 ps.

The grid version of ASP is simple to implement but suffers from the fact that as the growing resin is a rigid solid of particles arranged on a regular lattice it may not be able to conform exactly to the ideal shape of the distending binding site. We have therefore also implemented a fluid version of the ASP procedure, illustrated in Figure 2. In this the particles are not constrained to a grid but can move freely. Carefully chosen LJ parameters ensure that the fluid coheres into a single droplet but does not have such a high surface tension that it has a strong tendency to adopt a spherical form, irrespective of the optimal cavity shape. In this situation, the process for adding new particles is different. Since there are no fixed receptive points that can be monitored, the addition of new particles takes place near the center of the growing fluid droplet. To enable this to occur in an energetically reasonable way, the new particle is grown in. This is achieved by gradually increasing its nonbonded interactions with other particles using an exponential scaling

$$U_i = \gamma \sum_j 4\varepsilon_{ij}\left[\left(\frac{\sigma_{ij}}{r_{ij}}\right)^{12} - \left(\frac{\sigma_{ij}}{r_{ij}}\right)^{6}\right] \quad (1)$$

$$\gamma = \gamma_0^{-n} \quad (2)$$

where $U_i$ is the scaled interaction energy between the new particle and the system, $\gamma$ is the scaling factor, and the sum is over all particles within the nonbonded cutoff radius. We set $\gamma_0$ to 2.0 and $n$ to 19 when the new particle is first inserted and then gradually decrease $n$ by one every 0.1 ps. Once $n$ reaches zero, addition of the next particle begins. Therefore, a new particle is added to the system every 2 ps.

Nonbonded parameters of 10 kcal/mol well depth and 1.4 Å for equilibrium distance were employed for interactions between the LJ particles. This value for the well depth was chosen as it corresponds to a parametrization for a LJ fluid which is deep within the liquid−vapor phase coexistence region,[7] thus ensuring cohesion of the fluid droplet. Since using standard mixing rules based upon this parametrization would result in very strong LJ particle-protein interactions, which may result in undesirable deformation of the protein of interest, the same interaction parameters between the LJ

particles and other atoms were used as in the grid version. The spacing of particles on the grid when the active site region is filled (Figure 2(a)) is also increased compared with that used in the grid-version, to 1.4 Å, to ensure that there are no steric clashed between LJ particles when the MD simulation is started.

**2.2. Simulation Methods.** The process of initializing and equilibrating the systems of interest were identical for both the grid- and fluid-versions of ASP.

Protein structures were obtained from the Protein Data Bank,[8] and any ligands, water molecules, and ions not of interest were removed from the structure. The systems then had hydrogen atoms added and were solvated using the TIP3P water model, taking care not to fill the region of interest (for example, the active-site region), and the systems were made electroneutral by adding counterions using the LeAP module of AMBER. Amino acids were described using the AMBER-99 force field,[9] with small molecules being described using the general AMBER force field.[10] The rectangular block of LJ particles was then overlaid over the structure, with the size of the grid sufficient to encompass the region of interest. Particles that did not clash with the protein were switched on, grid neighbors were marked as receptive, and the remainder were switched off.

Having prepared the system of interest ready for simulation, the following equilibration procedure was employed. During equilibration, and the following MD simulations, a cutoff distance of 10 Å for nonbonded interactions was employed, with the long-range electrostatic interactions being accounted for via the smooth particle mesh Ewald method. Initially two minimization steps were performed (both consisting of initially using the steepest decent method, following by the conjugate gradient method); first only the solvent was minimized, followed by a minimization of the whole system where only the LJ particles were held fixed for the grid-version of ASP. MD simulations were then started with a 1 fs time step using the canonical (constant-NVT) ensemble, with the SHAKE algorithm being used to constrain all bonds to hydrogen at equilibrium values. The first 115 ps of MD simulation was used to allow the systems to reach thermodynamic equilibrium, with the temperature gradually being ramped from 0 to 300 K and atomic restraints being reduced from 100 to 0 kcal/mol/Å$^2$.

Once the system had reached thermodynamic equilibrium, additional LJ particles are gradually inserted into the system. These particles were added to the system at a rate of one every 2 ps. Typical simulations we have performed add between 100 and 200 particles, i.e. a total simulation time of between 200 and 400 ps. During these simulations there are no explicit restraints placed upon any atoms within the system, with the exception of the LJ particles in the grid-version of ASP which were held fixed using the belly function in AMBER.

## 3. RESULTS AND DISCUSSION

**3.1. Application to Cytochrome P450cam.** One of the best-studied testbeds for investigating ligand binding site flexibility has been P450cam. Crystal structures reveal that the ligand binding site is entirely buried, and no entrance or exit channels for ligands are obvious. A number of specialized MD studies have been performed to examine the opening and closing motions of P450cam which allow a ligand to pass to or from the buried active site. As a result of these studies three main classes of routes have been defined according to the secondary structure elements surrounding clusters of trajectories at the protein surface. These have been named pathways (pw) pw1, pw2, and pw3. pw2 was further subclustered into five subclasses, pw2a−e, that share at least one secondary structure element. A review of these pathways can be found in ref 11.

In order to locate the egress pathways in P450 the Wade group developed the random expulsion molecular dynamics (REMD) method,[12] where there is an artificial randomly oriented force on the ligand, in addition to the standard MD force field. Using this method the probability of spontaneous ligand exit in the time range amenable to MD simulations is enhanced. This study identified the three distinct egress pathways and showed that pw2a was the most likely exit pathway, with exit via pw3 also being observed, but with a much lower probability. Exit via pw1 was observed very rarely.

The REMD method was not, however, designed to provide realistic activation barriers or ruption forces. To achieve this steered molecular dynamics simulations were performed on P450cam,[13] where the ligand was "dragged" along each pathway by an external force. Using this technique it was shown that pw2a is the major pathway for the exit of a ligand from the active site of P450cam. Subsequent steered MD studies upon other P450s[14,15] have also identified pw2 as the major pathway. That said, it should be noted that it has been proposed[16] that different pathways for access and egress will be observed between membrane-bound mammalian P450s and soluble P450s.

Figure 3 shows snapshots obtained during the application of both the grid (panels A−C) and fluid (panels D−F) versions of the ASP methodology to P450cam starting from an equilibrated structure obtained after the filling of the active site cavity with LJ particles on a 20*20*20 grid centered upon the center of the active site cavity. It is apparent from these snapshots that as more LJ particles are added to the system the method is expanding the active site cavity, such that larger ligands may be docked than would be possible in the apo structure. During the initial stages of the ASP procedure both methods behave similarly; the particles expand the active site cavity uniformly, and the cavity volume (Figure 4), calculated using the VIODOO software package,[17] increases linearly with the number of LJ particles inserted and is almost identical for both versions of ASP.

After the insertion of approximately 120 LJ particles (240 ps of simulation) the different methods result in different behavior. The fluid version requires a strong LJ−LJ particle interaction energy to ensure cohesion of the fluid, which results in the cavity continuing to expand after forcing a large scale rearrangement of the protein. The grid version, however, does not force the protein to make a large scale rearrangement and expands in directions of lower stress and starts to fill channels leading away from the active site (Figure 3c). The possibility of using ASP to locate entry/exit channels has therefore been investigated. Figure 5 shows a snapshot from a grid simulation where the LJ particles have filled pw2a, the primary exit channel identified previously,[12] and have come into contact with solvent. Two other exit channels were are also identified in ref 12, and grid particles

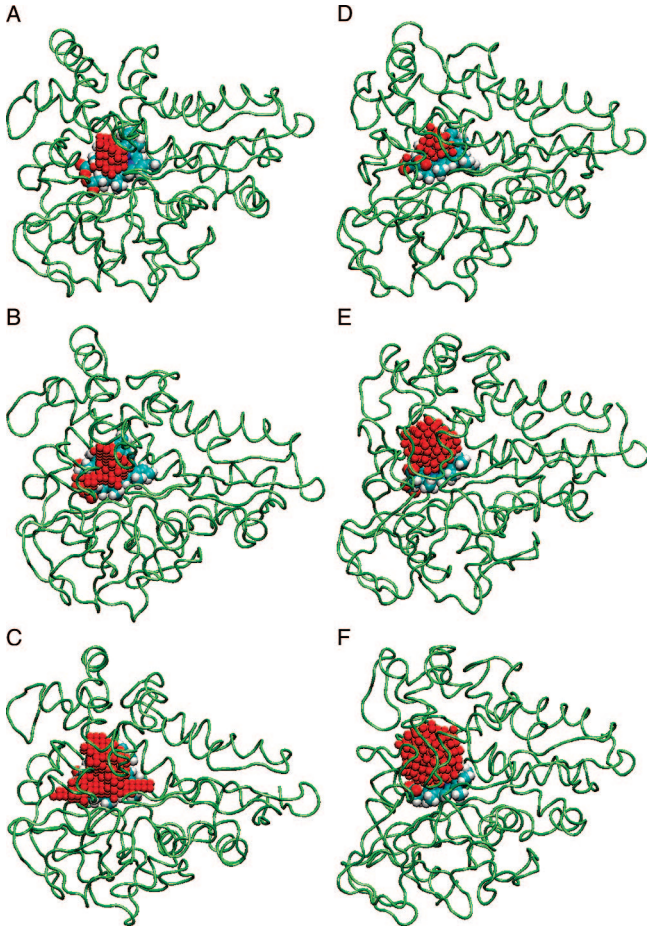


**Figure 3.** ASP applied in grid-based (panels A−C) and fluid-based (panels D−F) approaches to the investigation of cytochrome P450cam. Snapshots show the system after equilibration after filling the cavity with LJ particles (panels A and D), after the insertion of 100 LJ particles (panels B and E), and after the insertion of 200 LJ particles (panels C and F). For clarity, LJ particles are shown with a van der Waals radius smaller than that used during the simulation.

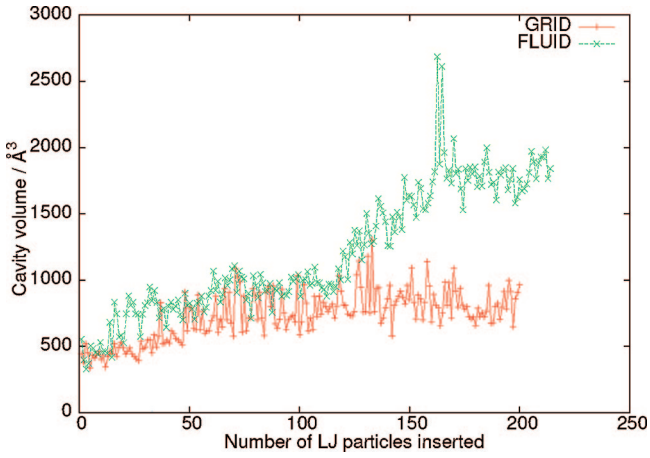


**Figure 4.** Growth in the volume of the active site cavity in P450cam through the course of grid-based and fluid-based ASP simulations.

also begin to fill these channels. The LJ particles also explore the xenon binding site located close to pw1;[11] however, the insertion of LJ particles into this binding site does not cause significant deformation of the protein structure. The possibility of using the fluid version to identify exit channels has also been investigated. To achieve this, the interactions

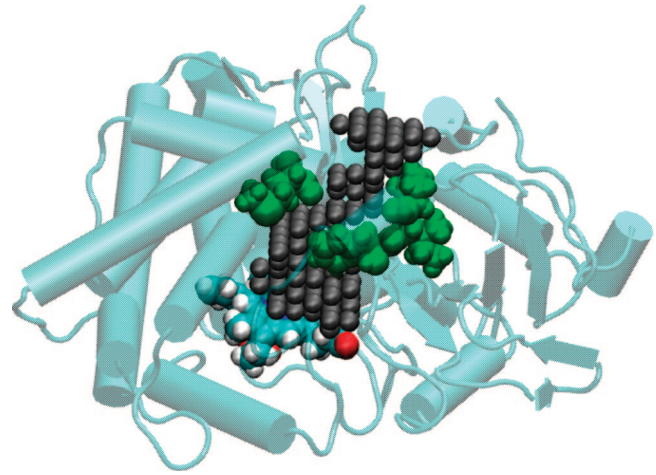

**Figure 5.** Snapshot from a grid-based ASP simulation where the insertion of 175 particles have forced the opening of the primary exit channel toward the top of the picture. Key protein residues lining this channel, PHE87, ILE88, ALA92, and LEU244, are shown in green. For clarity, LJ particles are shown with a van der Waals radius smaller than that used during the simulation.

between the LJ fluid and all other particles are made repulsive by setting the prefactor associated with the attractive $r^{-6}$ term in the LJ potential equal to zero, while leaving the prefactor associated with the repulsive $r^{-12}$ term unchanged from the parametrization described above. Using this model the active site cavity is filled with LJ particles until it reaches a critical size and is then expelled from the protein. By following the trajectory the fluid takes when leaving the protein exit channels may be identified. Using this method the fluid was observed to leave the protein along all three exit channels identified previously. That said, the ratio of pathways used differs in the present work, 6:3:1 (for pw1, 2 and 3 respectively), to that found previously, 4:7:3.[12] This difference is most likely due to the model not taking into account the chemical nature of ligands (i.e., a droplet of purely repulsive fluid as opposed to a molecule of camphor).

**3.2. Application to PcrA Helicase.** The PcrA helicase is a molecular motor that separates double-stranded DNA (ds-DNA) and is powered by ATP hydrolysis. Because of the availability of crystal structures of PcrA helicase in states both before and after ATP binding/hydrolysis, a particularly detailed view of the molecular mechanism of action of this motor protein is available, and modeling methods have been used to enhance this.[18–20] In the crystal structures PcrA is observed bound at the junction between the double- and single-stranded regions of a DNA fragment. One of the single-stranded DNA (ss-DNA) tails has a passive role and passes over the surface of the protein, while the other passes through a central channel, where it engages the motor machinery. However, because of the limited resolution of the crystal structure, only the first five bases of the seven in the channel were located, and as a result how the strand actually exits the protein remains unresolved. However, as discussed by Velankar et al.,[18] there is some additional very weak electron density on the outer surface of the protein, that can be interpreted as the disordered tail of DNA emerging from a narrow channel. As Figure 6 shows, near the last ss-DNA base, there are two possible channels. Because of the limited resolution of the X-ray structure, both appear partly open, but neither is large enough to readily accommodate a DNA strand. Channel 1, which is on the left, is formed by THR91, SER94, LEU540, ASN66, and THR65. Channel 2, which is on the right,

is formed by LYS67, THR65, ASN66, SER542, ASP543, and LEU544. ASN66 and THR65 are shared by these two channels. In this study, ASP was applied at the tail of the ss-DNA to study which channel is most likely to be the real DNA channel.

A grid containing 14*12*14 LJ particles with a spacing of 1.1 Å was created. The center of the box was placed near the 3′-terminus of the DNA strand. Because the region of interest here is not buried within the protein the ASP procedure is initiated by only turning on one particle located near the 3′-terminus of the DNA strand. After 200 ps of ASP simulation, 100 LJ particles had been distributed evenly in the region near channels 1 and 2, but none of them had actually entered either channel. However, the LJ particles were already beginning to indirectly affect these channels. The distance between the CA atoms on ASN66 and LEU540 roughly defines the radius of channel 1. At the beginning of the simulation this distance was 7.8 Å but had now increased to 9.2 Å. In the next phase of the simulation, ASP chose and exploited the channel with the lower resistance. After 200 LJ particles had been added, around 30 LJ particles had entered channel 1; however, none entered channel 2, and the ASN66-LEU540 distance was further increased to 9.9 Å. After 410 LJ particles had been added, around 96 of them now occupied channel 1, but channel 2 was still empty. The distance between ASN66 and LEU540 was now 9.8 Å. At this point the particles in channel 1 had reached the outside of the protein and had come into contact with the solvent (Figure 7). As the energy of expelling the solvent is much lower than further expanding the channels, ASP started to place particles outside of the protein instead of further expanding channel 1. In conclusion then, ASP provided clear evidence that channel 1, not channel 2, is the true route by which the ss-DNA tail exits the interior of the protein.

**3.3. Application to Glycogen Synthase Kinase 3*β* (GSK3*β*).** The ATP-binding pockets of protein kinases are now well-established as important drug targets.[21] Initial skepticism as to the possibility of designing selective inhibitors against a conserved binding site has proved to be, at least in part, misplaced. A large part of this stems from the observation that though all kinases bind ATP within a conserved site the flexibility of this site varies from kinase to kinase, so that ligands that bind with an element of induced fit can be selective. Extensive structural studies have revealed that one particular area of plasticity within the kinase fold is the Gly-rich P-loop. We hypothesized that applying ASP to kinases might be an interesting test of the method, to see if a) it could access biologically relevant binding modes and demonstrate the particular flexibility of this region as seen in X-ray structures and b) predict novel accessible conformations of the proteins that might be interesting alternative bases for selective drug design.

The grid-based version of ASP was used to study the inherent flexibility of the ATP-binding pocket of GSK3*β*. There is no high-resolution structure available of the apo-form of GSK3*β* in an unphosphorylated state; therefore, we began with a homology model[21] based on PDB code 1Q4L[22] in which the protein is bound to inhibitor I-5. Although it might be argued that this introduces a bias into the investigation, in fact this is not significant, as the conformation of the active site cavity in this modeled structure differs considerably from that observed in other GSK3*β* structures (see below). As ASP particles were inserted (on a 1.1 Å grid)

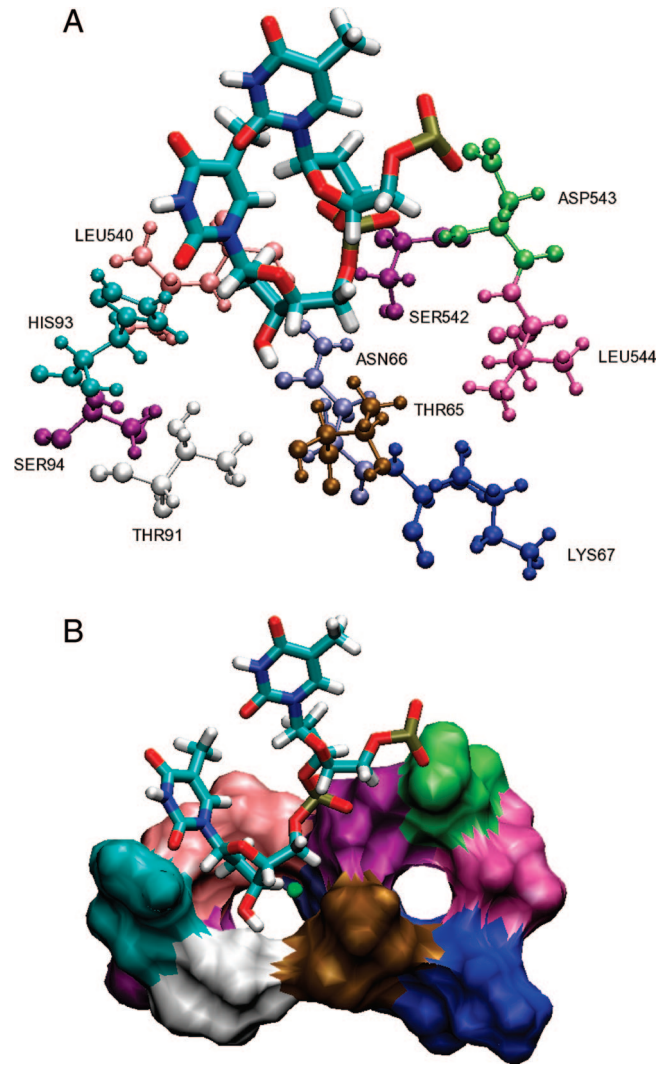


**Figure 6.** A: The DNA channels connecting the ss-DNA binding site to the outside of the protein. The last two DNA bases are colored by atom type, and the protein residues are represented as ball-and-stick models. Channel 1 is on the left and channel 2 is on the right. B: The first LJ particle (green sphere) near the last ss-DNA base in the substrate complex has been switched on by ASP.

into the binding site over a 400 ps time scale, the amino acid residues within the active site that constitute the Gly-rich P-loop underwent conformational change (Figure 8). This simulation resulted in the P-loop movement of more than 3.5 Å to accommodate the expanding mass of ASP particles. Very encouragingly, as the P-loop moves, it samples conformations that are significantly closer to those observed in the crystal structures of a variety of liganded complexes than is originally the case, but only once the ASP process has begun to exert significant pressure on the active site cavity, i.e., not until more ASP particles have been added than are required to fill the initial void (Table 1). Thus, the initial P-loop conformation has an rmsd of 3.88 Å from that observed in the crystal structure of the protein complexed with an indolylarylmaleimide inhibitor (PDB code 1R0E), but after 39 ASP particles have been added, this is reduced to 3.15 Å. By the time 53 ASP particles have been added, the P-loop conformation has adjusted further to more closely resemble that observed in the structures of GSK3*β* bound to both phosphate and inhibitor I-5 (PDB codes 1I09[23] and 1H8F,[24] respectively, rmsd reductions of 0.61 and 0.68 Å,

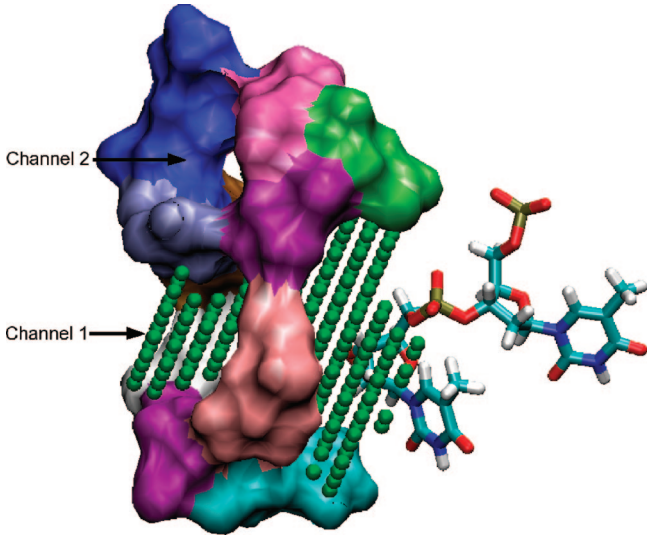


**Figure 7.** Side-view of the two channels after 410 LJ particles have been added. At this stage approximately 96 LJ particles have entered channel 1; however, none has entered channel 2. For clarity LJ particles are shown with a van der Waals radius smaller than that used during the simulation.

respectively). Finally, when 79 ASP particles have been added, the P-loop reaches a conformation considerably closer to that observed in the complex with staursporine (PDB code 1Q3D[22]) than is the case in the original model (rmsd reduced from 2.79 to 2.21 Å).

Conformational changes different than those typically observed upon ATP binding were also evident during the simulation. Distinct pockets within the ATP-binding site opened up in response to the growing mass of ASP particles, and as a consequence residues distal to the active site also underwent conformational change by more than 7.5 Å from their original positions as a result of ASP.

In conclusion, when applied to GSK3$\beta$, ASP gives very encouraging results. The pressurization procedure not only produces conformations of the active site that recapitulate known ligand-induced conformations but also identifies other, low-energy conformations of the protein that novel ligands could be designed to target. Current work is now exploiting this information.[25]

## 4. CONCLUSIONS

ASP provides a simple and unbiased way of generating novel, energetically reasonable protein conformations that may be better representations of the ligand binding conformation than an apo-form, when this is the only known structure. But even when a ligand-bound form is known, ASP could be valuable for lead hopping, revealing alternative modes of deformation, and so opportunities to interact with novel ligand scaffolds. ASP also has potential in other areas. In addition to the example of revealing hidden exit and entrance tunnels described above, we are studying how ASP may enable the ligand binding sites of homologous proteins, apparently very similar in a static sense, to be distinguished by their differing deformabilities, thus revealing unexpected opportunities for the development of selective ligands. The two current implementations of ASP, grid-based and fluid-based, may have slightly different, but overlapping, areas of optimal applicability. The grid-based approach is somewhat more controllable, and the user-chosen grid size and position limit the region that will be explored in a way that the fluid version cannot do. The fluid version however can respond to changes in the binding site cavity in a more flexible way than the grid based version can, so for example if an expansion of one region of the site requires a slight compensatory constriction in another, the fluid version can handle this while the grid version cannot (once a particle is switched on, it remains on). The cast itself is also a potentially valuable tool in virtual screening. In particular in its grid form, we are currently investigating how the information about restoring forces exerted by the protein on the pressurized cast that are encoded in the final set of receptive points that coat the surface may be valuable additions to QSAR-based screening methods.

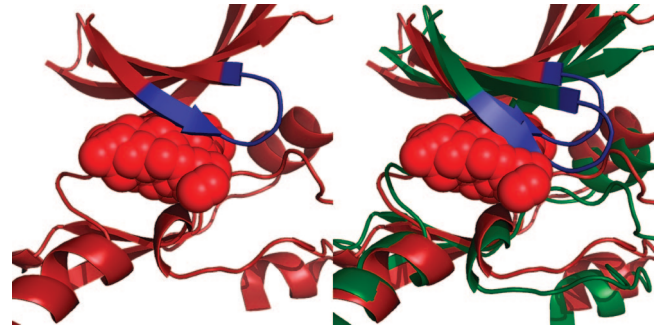

**Figure 8.** Left: closeup of GSK3$\beta$ active site after pressurization with 150 LJ particles spaced at 1.1 Å using the grid-based version of ASP. Right: comparison of the structures of the ligand-binding site before (green) and after (red) ASP, showing the observed movement in the P-loop (blue).

**Table 1.** RMDs (Å) of the Heavy Atoms of Residues 37−47, Which Includes the P-Loop, of GSK3$\beta$ Observed during the ASP Simulation, with respect to Four X-ray Crystal Structures of GSK3$\beta$-Ligand Complexes[a]

| | X-ray crystal structure | | | |
|---|---|---|---|---|
| | 1R0E | 1H8F | 1I09 | 1Q3D |
| active site empty | 3.88 | 2.78 | 2.97 | 2.79 |
| active site filled | 3.46 | 2.56 | 2.73 | 2.59 |
| active site optimally pressurized | 3.15 | 2.10 | 2.36 | 2.21 |
| optimal number of particles | 39 | 53 | 53 | 79 |

[a] Shown are the RMSDs at the start of the simulation where 1 particle is present, when the active site is just filled (17 particles added), and the minimum RMSD achieved during pressurization, along with the corresponding number of ASP particles added.

## ACKNOWLEDGMENT

We gratefully acknowledge the High Performance Computing facility at the University of Nottingham for providing CPU time.

**Supporting Information Available:** Patch file to implement ASP in AMBER7,[5] installation instructions, file usage, and details of additional input variables and file formats. This material is available free of charge via the Internet at http://pubs.acs.org.

## REFERENCES AND NOTES

(1) Sousa, S. F.; Fernandes, P. A.; Ramos, M. J. Protein-Ligand Docking: Current Status and Future Challenges. *Proteins* **2006**, *65*, 15–26.

(2) Meager, K. L.; Carlson, H. A. Incorporating protein flexibility in structure-based drug discovery: using HIV-1 protease as a test case. *J. Am. Chem. Soc.* **2004**, *126*, 13276–1328.
(3) Osterber, F; Morris, G. M.; Sanner, M. F.; Olson, A. J.; Goodsell, D. S. Automated docking to multiple target structures: incorporation of protein mobility and structural water heterogeneity in AutoDock. *Proteins* **2002**, *46*, 34–40.
(4) Goodfellow, J. M.; Knaggs, M.; Williams, M. A.; Thornton, J. M. Modelling protein unfolding: A solvent insertion protocol. *Faraday Discuss.* **1996**, *103*, 339–347.
(5) Case, D. A.; Pearlman, D. A.; Caldwell, J. W.; Cheatham , T. E., III; Wang, J.; Ross, W. S.; Simmerling, C. L.; Darden, T. A.; Merz, K. M.; Stanton, R. V.; Cheng, A. L.; Vincent, J. J.; Crowley, M.; Tsui, V.; Gohlke, H.; Radmer, R. J.; Duan, Y.; Pitera, J.; Massova, I.; Seibel, G. L.; Singh, U. C.; Weiner P. K.; Kollman P. A. *AMBER 7*; University of California: San Francisco, 2007.
(6) Allen, M. P.; Tildesley, D. J. *Computer Simulation of Liquids*; Clarendon: Oxford, United Kingdom, 1987.
(7) Smit, B. Phase diagrams of Lennard-Jones fluids. *J. Chem. Phys.* **1992**, *96*, 8639–8640.
(8) RCSB Protein Data Bank. http://www.pdb.org (accessed Mar 14, 2007).
(9) Wang, J. M.; Cieplak, P.; Kollman, P. A. How well does a restrained electrostatic potential (RESP) model perform in calculating conformational energies of organic and biological molecules? *J. Comput. Chem.* **2000**, *21*, 1049–1074.
(10) Wang, J. M.; Wolf, R. M.; Caldwell, J. W.; Kollman, P. A.; Case, D. A. Development and testing of a general amber force field. *J. Comput. Chem.* **2004**, *25*, 1157–1174.
(11) Wade, R. C.; Winn, P. J.; Schlichting, E.; Sudarko, A. survey of active site access channels in cytochromes P450. *J. Inorg. Biochem.* **2004**, *98*, 1175–1182.
(12) Lüdemann, S. K.; Lounnas, V.; Wade, R. C. How do substrates enter and products exit the buried active site of cytochrome P450cam? 1. Random expulsion molecular dynamics investigation of ligand access channels and mechanisms. *J. Mol. Biol.* **2000**, *303*, 797–811.
(13) Lüdemann, S. K.; Lounnas, V.; Wade, R. C. How do substrates enter and products exit the buried active site of cytochrome P450cam? 2. Steered molecular dynamics and adiabatic mapping of substrate pathways. *J. Mol. Biol.* **2000**, *303*, 813–830.
(14) Li, W. H.; Liu, H.; Scott, E. E.; Grater, F.; Halpert, J. R.; Luo, X. M.; Shen, J. H.; Jiang, H. L. Possible pathway(s) of testosterone egress from the active site of cytochrome P4502B1: A steered molecular dynamics simulation. *Drug Metab. Dispos.* **2005**, *33*, 910–919.
(15) Li, W. H.; Liu., H.; Luo, X. M.; Zhu, W. L.; Tang, Y.; Halpert, J. R.; Jiang, H. L. Possible pathway(s) of metyrapone egress from the active site of cytochrome P450 3A4: A molecular dynamics simulation. *Drug Metab. Dispos.* **2007**, *35*, 689–696.
(16) Schleinkofer, K.; Sudarko, A.; Winn, P. J.; Lüdemann, S. K.; Wade, R. C. Do mammalian cytochrome P450s show multiple ligand access pathways and ligand channelling? *Embo Rep.* **2005**, *6*, 584–589.
(17) Kleywegt, G. J.; Jones, T. A. Detection, delineation, measurement and display of cavities in macromolecular structures. *Acta Crystallogr., Sect. D: Biol. Crystallogr.* **1994**, *D50*, 178–185.
(18) Velankar, S. S.; Soultanas, P; Dillingham, M. S.; Subramanya, H. S.; Wigley, D. B. Crystal structures of complexes of PcrA DNA helicase with a DNA substrate indicate an inchworm mechanism. *Cell* **1999**, *97*, 75–84.
(19) Cox, K.; Watson, T.; Soultanas, P.; Hirst, J. D. Molecular Dynamics Simulations of a Helicase. *Proteins* **2003**, *52* (2), 254–262.
(20) Yu, J.; Ha, T.; Schulten, K. Structure-based Model of the Stepping Motor of PcrA Helicase. *Biophys. J.* **2006**, *91*, 2097–2114.
(21) Mazanetz, M. P.; Fischer, P. M. Untangling tau hyperphosphorylation in drug design for neurodegenerative diseases. *Nat. Rev. Drug Discovery* **2007**, *6*, 464–479.
(22) Bertrand, J. A.; Thieffine, S.; Vulpetti, A.; Cristiani, C.; Valsasina, B.; Knapp, S.; Kalisz, H. M.; Flocco, M. Structural Characterization of the GSK-3 Active Site Using Selective and Non-selective ATP-mimetic Inhibitors. *J. Mol. Biol.* **2003**, *33*, 393–407.
(23) ter Haar, E.; Coll, J. T.; Austen, D. A.; Hsiao, H. M.; Swenson, L.; Jain, J. Structure of GSK3beta reveals a primed phosphorylation mechanism. *Nat. Struct. Biol.* **2001**, *8*, 593–596.
(24) Dajani, R.; Fraser, E.; Roe, S. M.; Young, N.; Good, V.; Dale, T. C.; Pearl, L. H. Crystal structure of glycogen synthase kinase 3 beta: structural basis for phosphate-primed substrate specificity and auto-inhibition. *Cell* **2001**, *105*, 721–732.
(25) Mazanetz, M. P.; Withers, I. M.; Laughton, C. A.; Fischer, P. M. Exploiting Glycogen Synthase Kinase-3$\beta$ Flexibility in Molecular Recognition. *Biochem. Soc. Trans.* **2008**, *361*, 55–58.

CI7004725